# Supporting Information

# Fe doped $Ni_5P_4$ nanosheet arrays with rich P vacancies *via* phase transformation for efficient overall water splitting

*Junlei Qi,[1] Tianxiong Xu,[1] Jian Cao*,[1] Shu Guo*,[2] Zhengxiang Zhong*,[3] Jicai Feng[1]*

## 1. Experimental Section

***Fabrication of NiFe-LDH nanosheets:*** Firstly, we heated the carbon paper (CP) to 500 $^{o}$C for 2 h in a muffle furnace.Then, we dissolved 0.87 g $Ni(NO_3)_2 \cdot 6H_2O$, 0.135 g $Fe(NO_3)_3 \cdot 9H_2O$, 0.33 g $NH_3F$ and 0.9 g urea into 60 mL deionized water. After that, we put a piece of clean carbon paper into a 100 mL Teflon-lined stainless steel autoclave with the prepared solution, and heated the steel autoclave to 120 $^{o}$C for 6 h. Finally, we washed the obtained carbon papers with NiFe-LDH nanosheet arrays by deionized water and ethanol for several time, and dried them at 60 $^{o}$C overnight.

***Fabrication of $NiSe_2$|Fe nanosheets:*** We heated the obtained NiFe-LDH nanosheets to 450 $^{o}$C in a tube furnace under flowing Ar of 50 sccm, with 0.5g Se at 400 $^{o}$C in the upsteam, and maintained that for 1 h.

***Fabrication of D-$Ni_5P_4$|Fe nanosheets:*** The D-$Ni_5P_4$|Fe-2, 2.5, 3, 3.5 samples were obtained in the following way. We heated the obtained $NiSe_2$|Fe nanosheets to 400 $^{o}$C in a tube furnace under flowing Ar, with 0.5g $NaH_2PO_2 \cdot H_2O$ in the upsteam as phosphorus source, and maintained that for different time (2 h, 2.5 h, 3 h, 3.5 h). The obtained samples were denoted as D-$Ni_5P_4$|Fe-2, 2.5, 3, 3.5 according to the corresponding time. The optimal sample was D-$Ni_5P_4$|Fe-3, shortly denoted as D-$Ni_5P_4$|Fe.

***Fabrication of $Ni_5P_4$|Fe nanosheets:*** We obtained the $Ni_5P_4$|Fe nanosheets in the same way of fabricating D-$Ni_5P_4$|Fe by using NiFe-LDH as substitute.

## 2. Sample characterization

We use transmission electron microscope (TEM, Tecnai G2 F30), scanning electronic microscopy (SEM, Helios Nanolab 600i), X-ray photoelectron spectroscopy (XPS, Thermo Fisher) and X-ray diffraction (XRD, D8 Advance) to characterized the obtained samples.

## 3. Electrochemical measurements

All electrochemical performances were measured in the electrochemical workstation (CHI 760E). The HER and OER properties were measured in a three-electrode system. The obtained samples, carbon rod and Hg/HgO were used as working electrode, counter electrode and reference electrode, respectively. All the potential was converted to reversible hydrogen electrode. The scanning rate of polarization curves is 2 mV $s^{-1}$, and then we compensated the polarization curves with iR-correction. Before tests, all samples were cycled at 10 mV $s^{-1}$ until the stability of cyclic voltammetry (CV), then the data were collected. As a comparison, commercial Pt/C (20 wt% Pt) and $IrO_2$ were prepared on carbon paper, and the detailed process was referred to previous reseaches.[1, 2] After all the measurement, the calculation of Tafel slope was conducted in the following way. Firstly, for both HER and OER, the potential at 10 mA $cm^{-2}$ was read, shortly denoted as $E_{10}$. Next, an interval of about 0.04 V was selected around the $E_{10}$ to obtain the optimal linear relationship between Log j and E (j represents the current density and E represents the potential vs. RHE). Finally, the fitting slopes of samples were compared. Besides, we normalized the current density by using the ECSA value ($j_{ECSA}$=j/ECSA). The calculation formula of ECSA is as follows:

$$ECSA=(C_{dlsample}-C_{dlCP})/C_s$$

A specific capacitance ($C_s$) value of 0.040 mF/$cm^2$ in 1 M KOH was adopted. $C_{dlsample}$ and $C_{dlCP}$ refer to the the geometric double layer capacitance ($C_{dl}$) of sample and carbon paper.

## Reference

1. Y. Chen, Z. Ren, H. Fu, X. Zhang, G. Tian, H. Fu, *Small* 2018, **14**, 1800763.

2. X. Xiao, D. Huang, Y. Fu, M. Wen, X. Jiang, X. Lv, M. Li, L. Gao, S. Liu, M. Wang, C. Zhao, Y. Shen, *ACS Appl. Mater. Interfaces* 2018, **10**, 4689-4696.

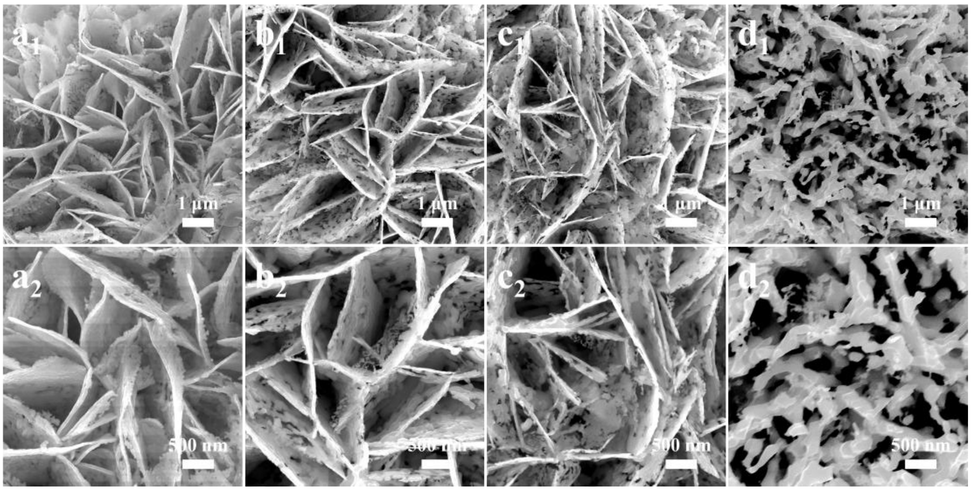


**Fig. S1** SEM images of (a) D-$Ni_5P_4$|Fe-2, (b) D-$Ni_5P_4$|Fe-2.5, (c) D-$Ni_5P_4$|Fe-3 and (d) D-$Ni_5P_4$|Fe-3.5.

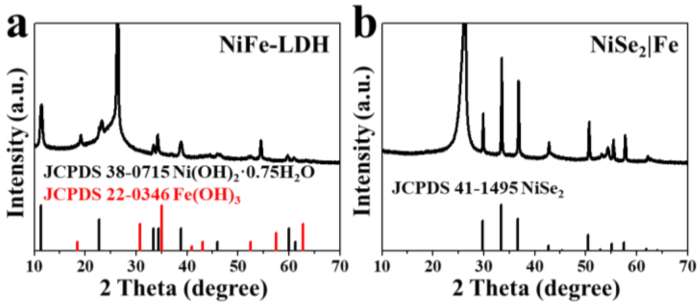


**Fig. S2** XRD patterns of (a) NiFe-LDH and (b) $NiSe_2$|Fe.

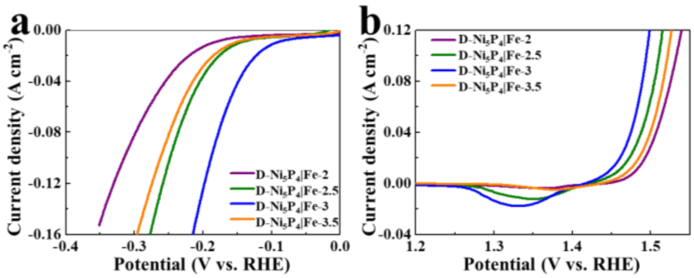


**Fig. S3** (a) HER and (b) OER performances of D-$Ni_5P_4$|Fe-2, 2.5, 3, 3.5.

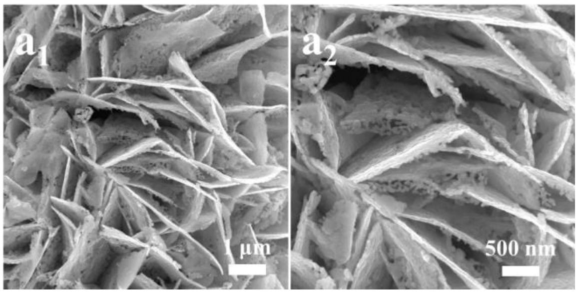


**Fig. S4** SEM images of D-$Ni_5P_4$|Fe after long time HER test.

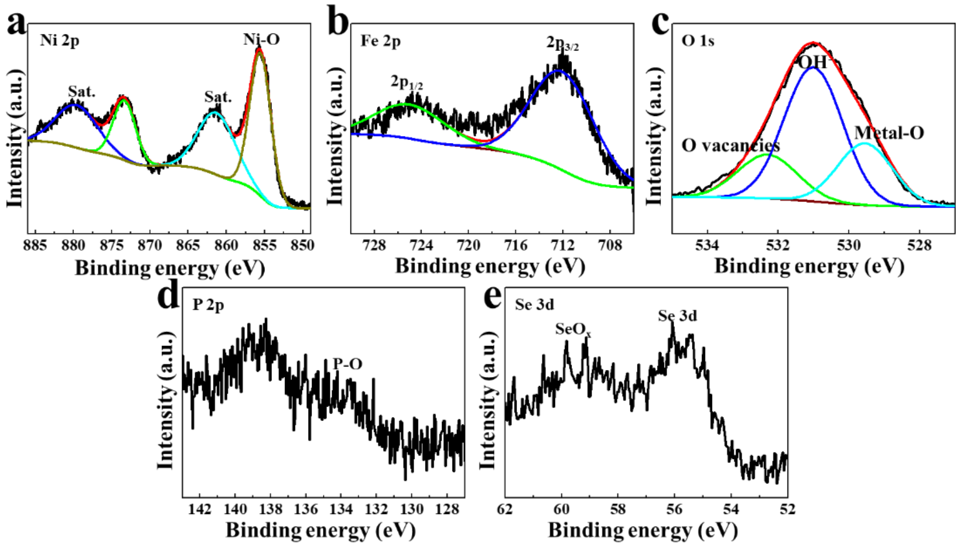


**Fig. S5** XPS (a) Ni 2p, (b) Fe 2p, (c) O 1s, (d) P 2p and (e) Se 3d spectra of D-$Ni_5P_4$|Fe after long time OER test.

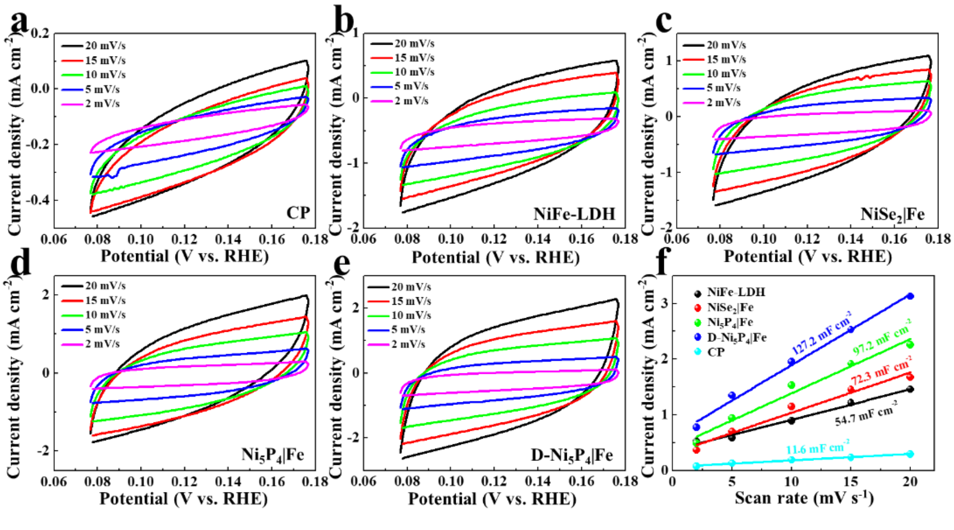


**Fig. S6** CV curves of obtained samples for estimating the $C_{dl}$ in HER tests..

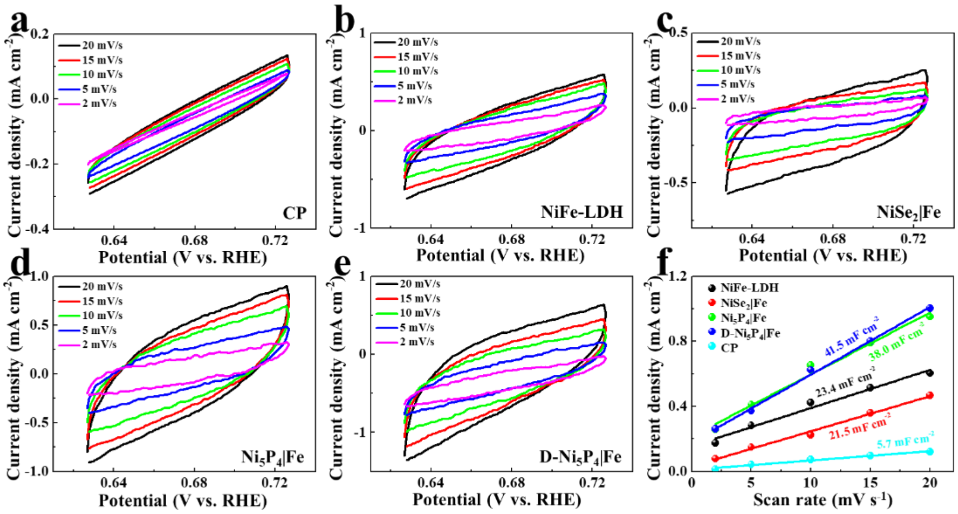


**Fig. S7** CV curves of obtained samples for estimating the $C_{dl}$ in OER tests.

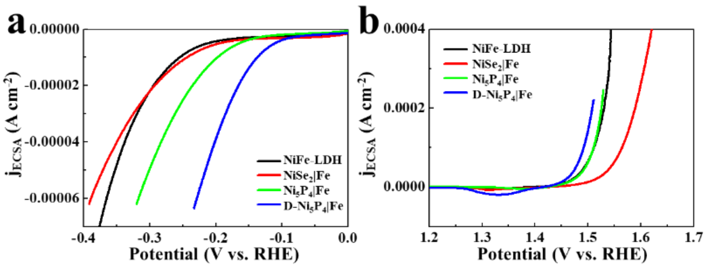


**Fig. S8** LSV curves normalized by $C_{dl}$ of obtained samples.

**Table S1** Comparison of HER performances for D-$Ni_5P_4$|Fe nanosheets with previsoulsy reported electrocatalysts in the alkaline media.

| Electrocatalyst | Substrate | Overpotential (mV) | Tafel slope (mV $dec^{-1}$) | Ref. |
|---|---|---|---|---|
| D-$Ni_5P_4$\|Fe | Carbon paper | 95 at 10 mA $cm^{-2}$ | 91.0 | **This work** |
| NiMoN | Carbon cloth | 109 at 10 mA $cm^{-2}$ | 95 | *Adv. Energy Mater.* 2016, **11**, 1600221. |
| N-$Ni_3S_2$/$VS_2$ | Ni foam | 151 at 10 mA $cm^{-2}$ | 107.5 | *Electrochim. Acta* 2018, **269**, 55 |
| Co-$Ni_3N$ | Carbon cloth | 194 at 10 mA $cm^{-2}$ | 156 | *Adv. Mater.* 2018, **13**, 1705516 |
| $Fe_{17.5\%}$-$Ni_3S_2$ | Ni foam | 142, 232 at 20, 100 mA $cm^{-2}$ | 95 | *ACS Catal*. 2018, **8**, 5431 |
| $(Ni_{0.33}Fe_{0.67})_2P$ | Ni foam | 214 at 50 mA $cm^{-2}$ | 73.2 | *Adv. Funct. Mater.* 2017, **37**, 1702513 |
| $NiMoP_2$ | Carbon cloth | 199 at 10 mA $cm^{-2}$ | 112 | *J. Mater. Chem. A* 2017, **5**, 7197 |
| NiCoP nanocone | Ni foam | 104 at 10 mA $cm^{-2}$ | 54 | *J. Mater. Chem. A* 2017, **5**, 14828 |
| Ni-Co-P hollow nanobricks | Powder | 107 at 10 mA $cm^{-2}$ | 46 | *Energy Environ. Sci.* 2018, **11**, 872 |
| $Ni_{1.85}Fe_{0.15}P$ NSAs/NF | Ni foam | 106 at 10 mA $cm^{-2}$ | 89.7 | *ACS Appl. Mater. Inter* 2017, **9**, 26001 |
| CoSe film | Ti mesh | 121 at 10 mA $cm^{-2}$ | 84 | *Chem. Commun.* 2015, **51**, 16683 |
| $TiO_2$@$Co_9S_8$ core-branch arrays | Ni foam | 139 at 10 mA $cm^{-2}$ | 65 | *Adv. Sci.* 2018, **5**, 1700772 |
| NiFe LDH@NiCoP | Ni foam | 120 at 10 mA $cm^{-2}$ | 88.2 | *Adv. Funct. Mater.* 2018, **28**, 1706847. |

1. If not metioned specifically, all overpotentials were corrected with iR compensation. 2. If not metioned specifically, all electrocatalysts are directly synthesized on conductive substrates.

**Table S2** Comparison of OER performances for D-$Ni_5P_4$|Fe nanosheets with previsoulsy reported electrocatalysts in the alkaline media.

| Electrocatalyst | Substrate | Overpotential (mV) | Tafel slope (mV $dec^{-1}$) | Ref. |
|---|---|---|---|---|
| D-$Ni_5P_4$\|Fe | Carbon paper | 217 at 10 mA $cm^{-2}$ | 45.7 | **This work** |
| $Ni_3S_2$/$VS_2$ | Ni foam | 227 at 10 mA $cm^{-2}$ | 59.9 | *Electrochim. Acta* 2018, **269**, 55 |
| $CoS_2$ nanotube | Carbon cloth | 276 at 10 mA $cm^{-2}$ | 81 | *Nanoscale Horiz.* 2017, **2**, 342 |
| Hyperbranched NiCoP Arrays | Ni foam | 268 at 10 mA $cm^{-2}$ | 75 | *ACS Appl. Mater. Inter* 2018, **10**, 41237 |
| $Co_9S_8$/$Ni_3S_2$ | Ni foam | 227 at 10 mA $cm^{-2}$ | 46.5 | *Appl. Catal. B-Environ.* 2019, **253**, 246 |
| $CoP_2$/RGO | Glass carbon electrodes | 300 at 10 mA $cm^{-2}$ | 96 | *J. Mater. Chem. A* 2016, **4**, 4686-4690 |
| N-$NiMoO_4$/$NiS_2$ | Carbon cloth | 267, 335 at 10, 100 mA $cm^{-2}$ | 44.3 | *Adv. Funct. Mater.* 2019, **29**, 1805298 |
| $Co_5Mo_{1.0}O$ nanosheets | Ni foam | 270 at 10 mA $cm^{-2}$ | 54.4 | *Nano Energy* 2018, **45**, 448 |
| Co-$Ni_3N$ | Carbon cloth | 307 at 10 mA $cm^{-2}$ | 57 | *Adv. Mater.* 2018, **13**, 1705516 |
| plasma-assisted synthesized NiCoP | Ni foam | 280 at 10 mA $cm^{-2}$ | 87 | *Nano Lett.* 2016, **16**, 7718 |
| NiSe | Ni foam | 271, ~350, 380 at 10, 50, 100 mA $cm^{-2}$ | 80 | *J. Energy Chem.* 2017, **26**, 1217 |
| $Ni_3S_2$@$MoS_2$/FeOOH | Ni foam | 260 at 10 mA $cm^{-2}$ | 49 | *Appl. Catal. B* 2019, **244**, 1004 |

1.If not metioned specifically, all overpotentials were corrected with iR compensation. 2. If not metioned specifically, all electrocatalysts are directly synthesized on conductive substrates.

**Table S3** Comparison of water-splitting performances for D-$Ni_5P_4$|Fe nanosheets with previsoulsy reported electrocatalysts in the alkaline media.

| Electrocatalyst | Substrate | Potential | Ref. |
|---|---|---|---|
| D-$Ni_5P_4$\|Fe | Carbon paper | 1.60 V at 10 mA $cm^{-2}$ | **This work** |
| $NiCo_2P_2$/graphene quantum dot | Ti mesh | 1.61 V at 10 mA $cm^{-2}$ | *Nano Energy* 2018, **48**, 284 |
| N-$NiMoO_4$/$NiS_2$ | Carbon cloth | 1.60 V at 10 mA $cm^{-2}$ | *Adv. Funct. Mater.* 2019, **29**, 1805298 |
| $NiMoP_2$ nanowires | Carbon cloth | 1.67 V at 10 mA $cm^{-2}$ | *J. Mater. Chem. A* 2017, **5**, 7191 |
| $NiCo_2S_4$ nanorod arrays | Ni foam | 1.64V at 20 mA $cm^{-2}$ | *J. Power Sources* 2018, **402**, 116 |
| $Ni_2P$ | Ni foam | 1.63 V at 10 mA $cm^{-2}$ | *J. Energ. Chem.* 2017, **6**, 1196 |
| $CuCo_2O_4$-NWs | Ni foam | 1.61 V at 10 mA $cm^{-2}$ | *Adv. Funct. Mater.* 2016, **26**, 8555 |
| Ni/NiP//Ni/NiP | Ni foam | 1.61 V at 10 mA $cm^{-2}$ | *Adv. Funct. Mater.* 2016, **26**, 3314 |